



Diazotrophic Growth Allows *Azotobacter vinelandii* To Overcome the Deleterious Effects of a *glnE* Deletion

Florence Mus,^a Alex Tseng,^b Ray Dixon,^c John W. Peters^a

Institute of Biological Chemistry, Washington State University, Pullman, Washington, USA^a; Department of Chemistry and Biochemistry, Montana State University, Bozeman, Montana, USA^b; Department of Molecular Microbiology, John Innes Centre, Norwich, United Kingdom^c

ABSTRACT Overcoming the inhibitory effects of excess environmental ammonium on nitrogenase synthesis or activity and preventing ammonium assimilation have been considered strategies to increase the amount of fixed nitrogen transferred from bacterial to plant partners in associative or symbiotic plant-diazotroph relationships. The GlnE adenylyltransferase/adenylyl-removing enzyme catalyzes reversible adenylylation of glutamine synthetase (GS), thereby affecting the posttranslational regulation of ammonium assimilation that is critical for the appropriate coordination of carbon and nitrogen assimilation. Since GS is key to the sole ammonium assimilation pathway of *Azotobacter vinelandii*, attempts to obtain deletion mutants in the gene encoding GS (*glnA*) have been unsuccessful. We have generated a *glnE* deletion strain, thus preventing posttranslational regulation of GS. The resultant strain containing constitutively active GS is unable to grow well on ammonium-containing medium, as previously observed in other organisms, and can be cultured only at low ammonium concentrations. This phenotype is caused by the lack of downregulation of GS activity, resulting in high intracellular glutamine levels and severe perturbation of the ratio of glutamine to 2-oxoglutarate under excess-nitrogen conditions. Interestingly, the mutant can grow diazotrophically at rates comparable to those of the wild type. This observation suggests that the control of nitrogen fixation-specific gene expression at the transcriptional level in response to 2-oxoglutarate via NifA is sufficiently tight to alone regulate ammonium production at levels appropriate for optimal carbon and nitrogen balance.

IMPORTANCE In this study, the characterization of the *glnE* knockout mutant of the model diazotroph *Azotobacter vinelandii* provides significant insights into the integration of the regulatory mechanisms of ammonium production and ammonium assimilation during nitrogen fixation. The work reveals the profound fidelity of nitrogen fixation regulation in providing ammonium sufficient for maximal growth but constraining energetically costly excess production. A detailed fundamental understanding of the interplay between the regulation of ammonium production and assimilation is of paramount importance in exploiting existing and potentially engineering new plant-diazotroph relationships for improved agriculture.

KEYWORDS *Azotobacter vinelandii*, *glnE*, ammonium assimilation, nitrogen fixation, regulation, glutamine synthetase

The most common pathways of ammonium assimilation in bacteria are known to be mediated by two major pathways (1, 2): the glutamate dehydrogenase (GDH) pathway when the extracellular concentration of ammonium is high, and the glutamine synthetase (GS) and glutamate synthase (GOGAT) pathway at low ammonium concentrations. In addition, the alanine dehydrogenase (ADH) enzyme has also been suggested to be involved in ammonium assimilation in most methylotrophs (3). The GDH

Received 13 February 2017 Accepted 10 April 2017

Accepted manuscript posted online 21 April 2017

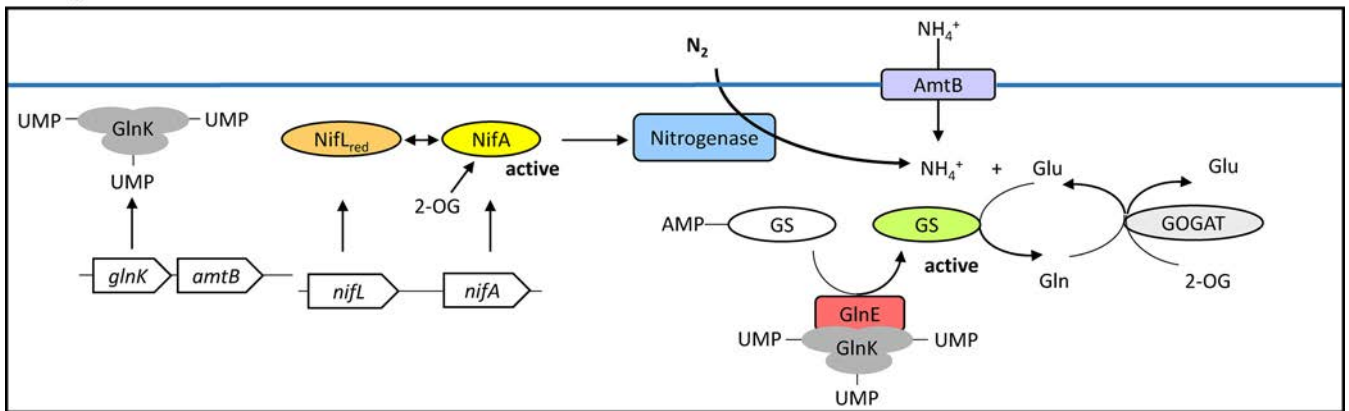
Citation Mus F, Tseng A, Dixon R, Peters JW. 2017. Diazotrophic growth allows *Azotobacter vinelandii* to overcome the deleterious effects of a *glnE* deletion. Appl Environ Microbiol 83:e00808-17. <https://doi.org/10.1128/AEM.00808-17>.

Editor M. Julia Pettinari, University of Buenos Aires

Copyright © 2017 American Society for Microbiology. All Rights Reserved.

Address correspondence to John W. Peters, john.peters.cab@gmail.com.

Nitrogen Limitation



Nitrogen Excess

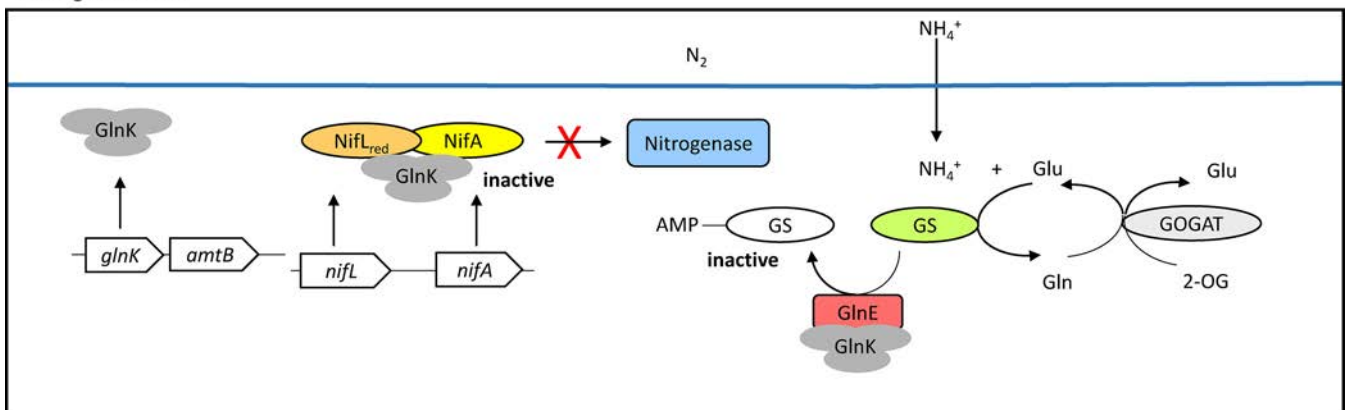


FIG 1 *A. vinelandii* has the NifL-NifA system, in which NifA activates transcription of *nif* genes and NifL modulates the activity of the transcriptional activator NifA in response to the presence of combined nitrogen and molecular oxygen. The nonuridylylated form of GlnK is required for NifL to inhibit NifA under conditions of nitrogen excess. Under conditions of nitrogen limitation, the binding of 2-oxoglutarate (2-OG) to NifA is required to prevent inhibition by NifL. In *A. vinelandii*, ammonium assimilation involves glutamine synthetase (GS) and glutamate synthase (GOGAT) enzymes. GS catalyzes the synthesis of glutamine (Gln) from ammonium and glutamate (Glu) in an ATP-dependent reaction. Both the synthesis and catalytic activity of GS are decreased under conditions of nitrogen excess and increased under conditions of nitrogen limitation. GS can be covalently modified with AMP groups, leading to a decrease in activity. This reaction is catalyzed by the bifunctional enzyme adenylyltransferase (GlnE) encoded by the *glnE* gene. The GlnK regulatory protein is also involved in this reaction by interacting with GlnE, thereby promoting GS adenylation. The deadenylation reaction is activated in the presence of a low level of glutamine. A high level of glutamine does the opposite. The unmodified form of GlnK activates GlnE, which adenylylates and inactivates GlnA, decreasing ammonium assimilation. GlnK activity is regulated by glutamine and 2-OG. The sensing of both molecules keeps the assimilation of nitrogen in balance with the rate of carbon assimilation. The AmtB (ammonium/methylammonium transport B) is essential for ammonium uptake. AmtB is encoded in the *glnK amtB* operon, whose expression is almost negligible in ammonium excess but is induced substantially when ammonium is limiting for growth. Under these conditions, ammonium is assimilated by the combined activities of glutamine synthetase and glutamate synthase.

pathway, which is present in many bacteria, catalyzes the reductive amination of 2-oxoglutarate (2-OG) by ammonium to give glutamate in an NADPH-dependent reaction. In the GS-GOGAT pathway, which is ubiquitous in bacteria, GS converts glutamate and ammonium to glutamine, and GOGAT transfers the amide group from glutamine to 2-OG to produce two glutamate molecules. The overall reaction is the production of glutamate from ammonium and 2-OG. The GOGAT pathway is energetically more costly than the GDH pathway, in that it consumes ATP.

In the nitrogen-fixing bacterium *Azotobacter vinelandii*, ammonium assimilation is thought to occur exclusively via the GS-GOGAT pathway (4) (Fig. 1). GS from *A. vinelandii* is biochemically very similar to the GS of other Gram-negative bacteria (5). However, regulation of GS expression appears to differ in some aspects from that of enteric bacteria, including *Escherichia coli*, *Salmonella enterica* serovar Typhimurium, *Klebsiella aerogenes*, and diazotrophic strains of *Klebsiella pneumoniae*, since the absolute amount of GS protein does not seem to vary with the nitrogen source in *A. vinelandii*. In enteric bacteria and diazotrophic strains of *Klebsiella pneumoniae*, the nitrogen regulatory (Ntr) system controls the transcription of the *glnA* gene (encoding

GS) and the activity of the GS. In contrast, expression of the *A. vinelandii glnA* gene requires neither *ntxA* (*rpoN*) nor *ntxC* function (6, 7). Although the synthesis of the enzyme is not repressed by NH_4^+ and/or a number of amino acids in the growth medium, the biosynthetic activity of the enzyme was rapidly lost through adenylylation in response to the addition of ammonium (8).

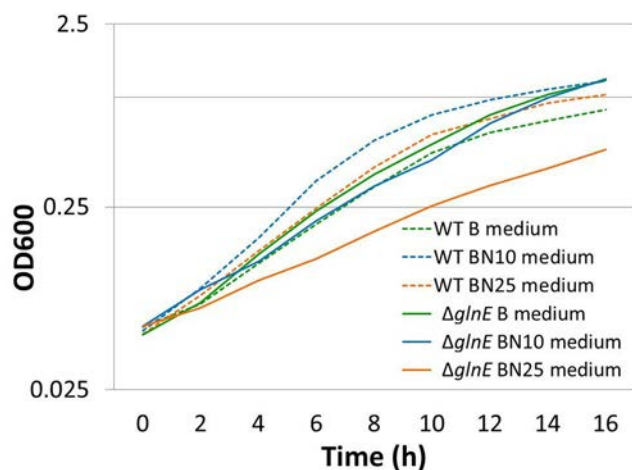
In most bacteria, GS activity is posttranscriptionally controlled by adenylylation (9) or oxidative modification (10, 11) in response to a multitude of extracellular and intracellular stimuli (12, 13). In *E. coli* and other bacteria, modification of GS by the covalent addition of AMP leads to a reduction in enzyme activity (12, 14, 15). Since the adenylyltransferase/adenylyl-removing enzyme encoded by *glnE* can catalyze both the addition and removal of AMP, it has a critical role in modulating GS activity in the cell. In *E. coli* and *Streptomyces coelicolor*, *glnE* seems not to be essential, and *E. coli* mutants can grow without supplements (16). However, high GS activity appears to cause a growth defect in many organisms under certain conditions. In *S. Typhimurium*, the elevated levels of GS activity in a *glnE* mutant cause transitory growth problems only upon an upshift in the nitrogen source (17). In *K. aerogenes*, the rate of synthesis of GS is controlled by the nitrogen source of the growth medium: it is high in media when the nitrogen source is growth rate limiting and low in media containing an excess of ammonium. The deletion of *glnE* in this organism prevents adenylylation of GS, resulting in constitutively high GS activity (18). In the diazotroph *K. pneumoniae*, the product of the *glnE* gene is responsible for both adenylylation and deadenylylation of GS, which results in inactivation or activation of the GS in response to fixed-nitrogen conditions. In this diazotroph, the *glnA* gene product plays an important role in ammonium assimilation, while it appears not to be required for expression of the *nif* regulon (19). In *A. vinelandii*, GlnA (Avin_45850) is a type I GS, and thus, its activity is expected to be regulated by the adenylyltransferase GlnE (Avin_44890) (20, 21) (Fig. 1), but little is known about the role of this enzyme in the regulation of ammonium assimilation and nitrogen fixation.

Overcoming the inhibitory effects of excess environmental ammonium on nitrogenase synthesis or activity and preventing ammonium assimilation have been considered strategies to increase the amount of fixed nitrogen transferred from bacterial to plant partner in associative or symbiotic plant-diazotroph relationships. Because the release of ammonium by soil diazotrophs, particularly those associated with roots, is of considerable agronomic interest, we have reinvestigated the role of the GS in nitrogen assimilation and nitrogen fixation in *A. vinelandii*.

In this study, we have generated a single-knockout mutant in a gene involved in the regulation of GS activity, namely, *glnE*. Correlations between enzyme activity levels, intracellular metabolite concentrations, and gene expression levels have been investigated in the *glnE* mutant strain. The resulting strain containing constitutively active GS is unable to grow well on ammonium-containing medium. The inability of the cells to adenylylate GS results in depletion of the 2-OG pool. However, the *glnE* mutant strain can grow diazotrophically at rates comparable to those of the wild type, suggesting that the control of nitrogen fixation-specific gene expression at the transcriptional level in response to 2-OG is sufficiently tight to regulate ammonium production at appropriate levels for optimal carbon and nitrogen balance. The *glnE* mutant strain can be used as a tool to examine the threshold of ammonium required and/or tolerated under a specific set of growth conditions and to select for mutant strains with higher titers of ammonium tolerance.

RESULTS

Phenotype of *glnE* mutant strain. A wild-type strain and *glnE* mutant strain were cultured in liquid medium under diazotrophic conditions (B medium) and under nondiazotrophic conditions in the presence of 10 and 25 mM NH_4^+ acetate (BN10 medium and BN25 medium, respectively) (Fig. 2). The *glnE* mutation had no significant effect on cell growth under diazotrophic conditions. The wild-type strain and *glnE* mutant strain grow at similar rates (growth rate, 0.25 optical density at



	B medium		BN10 medium		BN25 medium	
	μ	D	μ	D	μ	D
WT	0.25 +/- 0.023	4.0 +/- 0.37	0.34 +/- 0.039	2.96 +/- 0.35	0.27 +/- 0.031	3.66 +/- 0.36
$\Delta glnE$	0.25 +/- 0.006	4.0 +/- 0.095	0.22 +/- 0.016	4.60 +/- 0.32	0.16 +/- 0.01	6.23 +/- 0.21

FIG 2 Growth curves of the wild-type strain and *glnE* mutant strain under diazotrophic conditions (B medium) and excess- NH_4^+ acetate conditions (BN10 medium, 10 NH_4^+ acetate; BN25 medium, 25 mM NH_4^+ acetate). Cells were grown aerobically in 500-ml Erlenmeyer flasks, which contained 200 ml of Burk's sucrose medium in the absence or presence of NH_4^+ acetate, incubated at 30°C on a rotary shaker at 180 rpm. The results show the mean and standard deviation for data from triplicate experiments. The table summarizes the growth characteristics of the wild-type strain and the *glnE* mutant strain under the different growth conditions: growth rate (μ , in OD_{600} per hour) and generation time (D, in hours).

600 nm [$\text{OD}_{600}] \cdot \text{h}^{-1}$), with a generation time of 4 h (Fig. 2). When cells were cultured in the presence of 10 and 25 mM NH_4^+ acetate as a nitrogen source, the generation times of the *glnE* mutant cells appeared to increase compared to that observed under diazotrophic conditions. The generation times for the *glnE* mutant strain were estimated to be 4.6 h under 10 mM NH_4^+ acetate conditions and 6.2 h under 25 mM NH_4^+ acetate conditions. On the other hand, the doubling times for the wild-type cells in the presence of 10 and 25 mM NH_4^+ acetate appeared to decrease compared to that observed under diazotrophic conditions. The generation times for the wild-type strain were estimated to be 3 h under 10 mM NH_4^+ acetate conditions and 3.6 h under 25 mM NH_4^+ acetate conditions.

Phenotypic characteristics of the wild-type strain and *glnE* mutant strain were analyzed on agar plates supplemented with different concentrations of nitrogen and carbon sources. Under diazotrophic conditions, the *glnE* mutant strain exhibited a growth phenotype similar to that of the wild-type strain (Fig. 3). However, the *glnE* mutant strain showed a growth defect phenotype compared to the wild-type strain when using 25 mM NH_4^+ acetate as the nitrogen source (Fig. 3). This growth defect was not observed on cells grown on medium supplemented with sodium acetate (Fig. 3).

Effect of MSX on growth and metabolite pools. The GS inhibitor methionine sulfoximine (MSX) provides a useful probe to analyze the influence of GS activity on growth and metabolism (22, 23). The effect of this GS inhibitor has been investigated on growth and intracellular metabolite contents for both strains under nondiazotrophic conditions. High NH_4^+ acetate concentrations (25, 50, and 100 mM) were used in these experimental setups, since the *glnE* mutant strain appeared to show a profound growth defect in liquid culture when 25 mM NH_4^+ acetate was used as a fixed nitrogen source.

The wild-type strain and the *glnE* mutant strain were grown on agar plates supplemented with NH_4^+ acetate at different concentrations (0, 25, 50, and 100 mM) in the presence or absence of 1 mM MSX. The growth of the wild-type strain was moderately sensitive to MSX when using NH_4^+ acetate as the nitrogen source. On the other hand, the *glnE* mutant strain exhibited a major difference in sensitivity to MSX under excess-ammonium conditions, since the growth defect of the *glnE* mutant strain

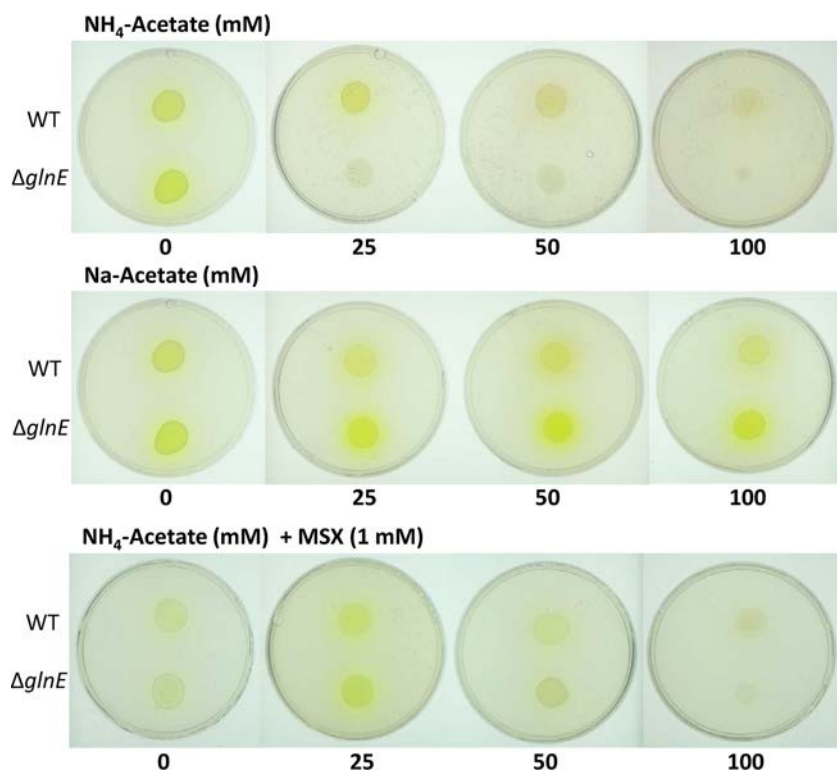


FIG 3 Phenotypic characteristics of wild-type (WT) strain and *glnE* mutant strain ($\Delta glnE$) on B medium agar plates supplemented with different concentrations of NH_4^+ acetate (0, 25, 50, and 100 mM; top row) and sodium acetate (0, 25, 50, and 100 mM; middle row) and at different concentrations of NH_4^+ acetate (0, 25, 50, and 100 mM) in the presence of MSX (1 mM; bottom row).

observed on agar plates in the absence of MSX was abolished when MSX was present (Fig. 3).

Pools of intracellular metabolites (glutamine, glutamate, and 2-OG) were measured on MSX-treated cells after the addition of NH_4^+ acetate. Cells were cultured under diazotrophic conditions until mid-exponential phase (OD_{600} 0.5) and subjected to an ammonium shock (25 mM NH_4^+ acetate) for 3 h. The presence of MSX prevented the accumulation of intracellular glutamine in *glnE* mutant cells but resulted in high 2-OG levels in the wild-type and gradual accumulation of 2-OG in the *glnE* mutant strain. In contrast, the presence of MSX did not significantly change the intracellular glutamate pool in the *glnE* mutant strain (Fig. 4).

GS activity and nitrogenase activity in *glnE* mutant strain upon NH_4^+ acetate addition. Glutamine synthetase (GS) activity was measured in the wild-type strain and *glnE* mutant strain using the biosynthetic assay described in Materials and Methods (Fig. 5A). Cells were cultured under diazotrophic conditions until mid-exponential phase (OD_{600} 0.5) and subjected to an ammonium shock (10 mM NH_4^+ acetate) for 300 min. The same cultures were analyzed for nitrogenase activity (Fig. 5B). The concentration of 10 mM NH_4^+ acetate was used in these ammonium shock experiments, since this concentration seemed to be less damaging for the cells over the time course of the experiment than the 25 mM NH_4^+ acetate concentration.

The biosynthetic GS assay was carried out to measure active GS, as described in Materials and Methods. The *glnE* mutant strain showed a level of biosynthetic GS activity identical to that of the wild-type strain prior to the NH_4^+ acetate shift (Fig. 5A). In response to an increase in NH_4^+ acetate concentration, the biosynthetic GS activity decreased over time in the wild-type strain (Fig. 5A). In the *glnE* mutant strain, the biosynthetic GS activity remained unchanged after the NH_4^+ acetate shift (Fig. 5A).

Little difference in nitrogenase activity was observed between the wild-type strain and the *glnE* mutant strain under diazotrophic conditions (Fig. 5B). However, the

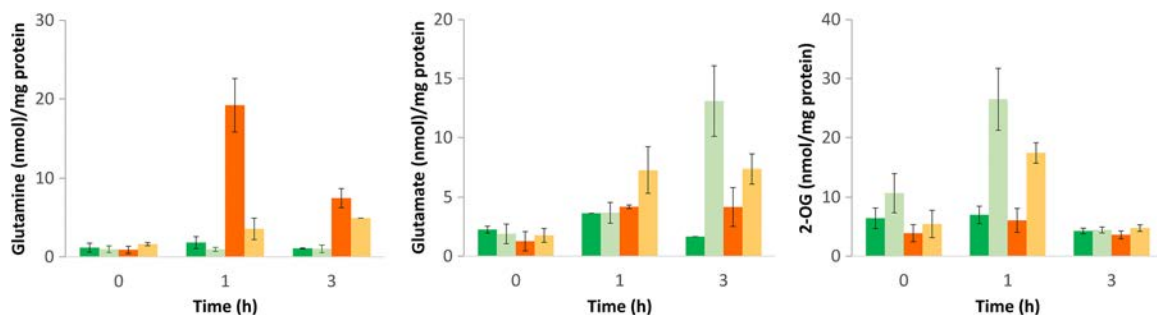


FIG 4 The effect of NH₄⁺ acetate addition on intracellular metabolite content in the presence of MSX. Bar graphs show the quantification of intracellular metabolites in the wild-type strain in the absence of MSX (dark-green bars), the wild-type strain in the presence of MSX (light-green bars), the *glnE* mutant strain in the absence of MSX (dark-orange bars), and the *glnE* mutant strain in the presence of MSX (light-orange bars). The changes in intracellular metabolite levels (glutamine, glutamate, and 2-OG) following the exposure of the cells to 25 mM NH₄⁺ acetate in the absence and presence of MSX are presented as nanomoles metabolite per milligram of protein at indicated time points (0, 1, and 3 h) after the NH₄⁺ acetate addition. The results show the mean and standard deviation (error bars) for data from triplicate experiments.

nitrogenase activity of the *glnE* mutant strain dropped severely within 5 min after the 10 mM NH₄⁺ acetate shift, whereas the activity of the wild-type strain decreased progressively and remained significant within 15 min after the shift (Fig. 5B).

Changes in transcript abundance upon addition of NH₄⁺ acetate. Real-time reverse transcription-PCR (RT-PCR) analyses were performed to examine the effects of NH₄⁺ acetate shock (10 mM NH₄⁺ acetate) on transcript abundance in the wild-type strain and *glnE* mutant strain. Transcripts encoding GlnA and NifH were examined (see Fig. S2 in the supplemental material). For these experiments, the concentration of 10 mM NH₄⁺ acetate was preferred over the concentration of 25 mM NH₄⁺ acetate, since 25 mM NH₄⁺ acetate appeared to be damaging to the cells.

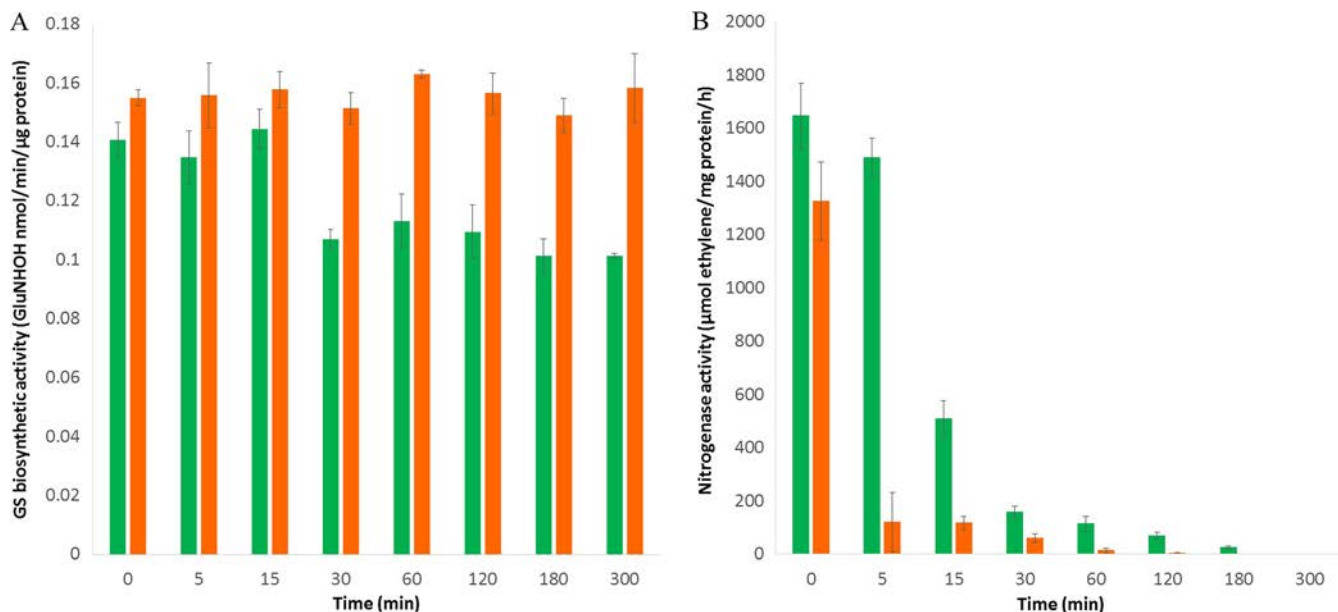


FIG 5 The effect of NH₄⁺ acetate addition on GS activity and nitrogenase activity. (A) Bar graphs show the changes in biosynthetic GS activity in wild-type strain (dark green bars) and *glnE* mutant strain (dark orange bars). The changes in biosynthetic GS activity following exposure of the cells to 10 mM NH₄⁺ acetate are presented as nanomoles γ -glutamyl hydroxamate (GluNHOH) per minute per microgram of protein at indicated time points (0, 5, 15, 30, 60, 120, 180, and 300 min) after the NH₄⁺ acetate addition. The results show the mean and standard deviation (error bars) for data from triplicate experiments. (B) Bar graphs show the changes in nitrogenase activity in wild-type strain (dark-green bars) and *glnE* mutant strain (dark-orange bars). The changes in nitrogenase activity following exposure of the cells to 10 mM NH₄⁺ acetate are presented as micromoles ethylene per milligram of protein per hour at indicated time points (0, 5, 15, 30, 60, 120, 180, and 300 min) after NH₄⁺ acetate addition. The results show the mean and standard deviation (error bars) for data from triplicate experiments.

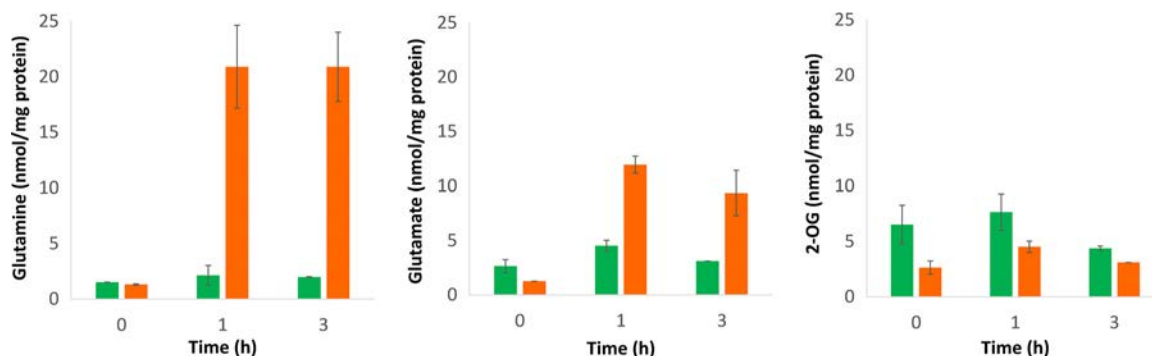


FIG 6 The effect of NH_4^+ acetate addition on intracellular metabolite content. Bar graphs show the quantification of intracellular metabolites in wild-type strain (dark-green bars) and *glnE* mutant strain (dark-orange bars). The changes in intracellular metabolite levels (glutamine, glutamate, and 2-OG) following exposure of the cells to 10 mM NH_4^+ acetate are presented as nanomoles metabolite per milligram of protein at indicated time points (0, 1, and 3 h) after the NH_4^+ acetate addition. The results show the mean and standard deviation (error bars) for data from triplicate experiments.

Steady-state *glnA* transcript levels were not significantly different in the wild-type strain and the *glnE* mutant strain prior to the addition of NH_4^+ acetate. After the addition of 10 mM NH_4^+ acetate, steady-state *glnA* transcript levels seemed to decrease in both strains. The *glnE* mutant strain and wild-type strain exhibited similar steady-state *nifH* transcript levels prior to the addition of NH_4^+ acetate. Under excess- NH_4^+ acetate conditions, steady-state *nifH* transcript levels decreased over time in both strains.

Influence of NH_4^+ acetate addition on metabolite levels. Intracellular and extracellular metabolite contents (glutamine, glutamate, and 2-OG) were measured in growing cells after the addition of 10 mM NH_4^+ acetate. This concentration was used for the upshift experiments, since 10 mM NH_4^+ acetate appeared not to be as damaging to the cells as 25 mM NH_4^+ acetate.

The glutamine pool in the *glnE* mutant strain was similar to that in the wild-type strain prior to the addition of NH_4^+ acetate. However, the intracellular pool of glutamine in the *glnE* mutant strain increased dramatically by at least 20-fold 1 h after NH_4^+ acetate addition and remained high 3 h after the ammonium upshift (Fig. 6). In comparison, intracellular glutamine increased only by a maximum of 2-fold after the ammonium upshift in the wild-type strain (Fig. 6). Additional measurements indicated that glutamine had been excreted in large amounts into the medium by the *glnE* mutant strain within 1 h after the addition of 10 mM NH_4^+ acetate and declined thereafter (Fig. S3).

Under diazotrophic conditions, the *glnE* mutant strain had approximately 50% of the intracellular glutamate content observed in the wild-type strain. Interestingly, the intracellular glutamate pool increased by 12-fold in the *glnE* mutant strain within 1 h after the addition of 10 mM NH_4^+ acetate and remained high up to 3 h after the ammonium upshift (Fig. 6). In the wild-type strain, intracellular glutamate content increased only by a maximum of 2-fold within 1 h after the addition of NH_4^+ acetate. The *glnE* mutant strain and the wild-type strain appeared to excrete significant levels of glutamate in the medium after the addition of NH_4^+ acetate (Fig. S3).

The intracellular 2-OG pool was significantly lower in the *glnE* mutant strain under diazotrophic conditions than in the wild-type strain. This difference was also maintained following addition of NH_4^+ acetate. However, both strains accumulated high levels of extracellular 2-OG after the upshift (Fig. S3).

In the experiments described above, the ratio of glutamine to 2-OG of the wild-type strain increased slightly after the addition of 10 mM NH_4^+ acetate, changing from 0.2 to about 0.4 (Fig. S4). In the *glnE* mutant strain, however, the ratio of glutamine to 2-OG increased dramatically. The ratio changed from 0.6 to 15 within 3 h after the addition of 10 mM NH_4^+ acetate (Fig. S4).

DISCUSSION

GS activity is tightly regulated at the transcriptional and posttranslational levels in many organisms, and high GS activity appears to cause growth problems under certain conditions. In *S. Typhimurium*, elevated levels of GS activity in *glnE* mutants lacking adenylyl transferase activity result in large growth defects, specifically upon the shift from a nitrogen-limited growth medium to medium containing excess ammonium (17). Although no significant growth defects were observed in a *glnE* mutant of *Rhodospirillum rubrum*, deliberate overexpression of GS in this background resulted in growth inhibition (24). Furthermore, the construction of *R. rubrum glnE* mutant strains can result in reduced GS activity as a consequence of secondary mutations that prevent GS overexpression in a *glnE* background (25). The *A. vinelandii glnE* deletion mutant characterized in this study exhibited significant growth impairment in media containing excess NH_4^+ acetate, and under these conditions, the level of active GS in the *glnE* mutant strain was significantly higher than that of the wild-type strain. Since the growth defect of the *glnE* mutant strain under excess- NH_4^+ conditions was abolished by the presence of the GS inhibitor (MSX), it seems likely that growth impairment results from high catalytic activity of GS in the absence of adenylylation.

The constitutive activity of GS in the *glnE* mutant strain resulted in a much higher increase in intracellular glutamine than that with the wild-type strain after the addition of NH_4^+ acetate (Fig. 7). This burst in glutamine synthesis was accompanied by excretion of high concentrations of glutamine into the medium. Similar observations were reported for *glnE* mutants of *S. Typhimurium* (17). As a consequence, the glutamine-to-glutamate ratio increased significantly in the *glnE* mutant strain from around 0.7 to 3.5 within 3 h after the addition of NH_4^+ acetate. In the wild-type strain, this ratio stayed unchanged (glutamine-to-glutamate ratio, around 0.6) after the addition of 10 mM NH_4^+ acetate. Glutamate is the most abundant metabolite in *E. coli* and is homeostatically maintained at fairly constant levels (26). We observed that the *A. vinelandii glnE* mutant strain excreted higher levels of glutamate into the medium than the wild-type strain, perhaps indicative of an attempt to maintain glutamate homeostasis.

The ratio of glutamine to 2-OG is a signal of the cellular nitrogen status in *E. coli*, with high ratios being indicative of nitrogen sufficiency and low ratios reflecting nitrogen limitation (27). Contrary to expectations, the intracellular 2-OG pool transiently increased in wild-type bacteria following the addition of NH_4^+ acetate and subsequently declined after 3 h, whereas a much smaller transient increase was observed in the *glnE* mutant strain. However, both strains excreted substantial amounts of 2-OG into the medium under these conditions, indicative of carbon overflow metabolism (28). The burst of glutamine synthesis in the *glnE* mutant strain following ammonium addition is likely to deplete the 2-OG pool as a consequence of carbon skeletons being drained through the GS/GOGAT pathway. However, carbon depletion is unlikely to be responsible for the growth phenotype of the *glnE* mutant strain in the presence of NH_4^+ acetate, as this strain is capable of excreting 2-OG under these conditions. The bifunctional activity of the GlnE enzyme is considered to robustly maintain the ratio of glutamine to 2-OG through the elaborate regulation of GS activity (29). Deletion of *glnE* in *A. vinelandii* abolishes this robustness, resulting in a dramatic shift in the ratio of glutamine to 2-OG as a consequence of excessive glutamine biosynthesis by GS. Under conditions of sudden NH_4^+ excess, the *glnE* mutant strain clearly appeared to be unable to regulate the ratio of glutamine to 2-OG (Fig. 7). The addition of the GS inhibitor MSX restored the ratio of glutamine to 2-OG in the *glnE* mutant strain to the levels observed in the wild-type strain and the conferred the ability to grow under excess- NH_4^+ conditions. We therefore propose that the growth phenotype of the *glnE* mutant strain in the presence of NH_4^+ arises either from glutamine toxicity or from the excessive biosynthesis of GS, which utilizes ATP as a substrate.

The regulation of ammonium assimilation in *A. vinelandii* is somewhat unusual, in that the expression of *glnA* (encoding GS) is not subject to regulation at the transcrip-

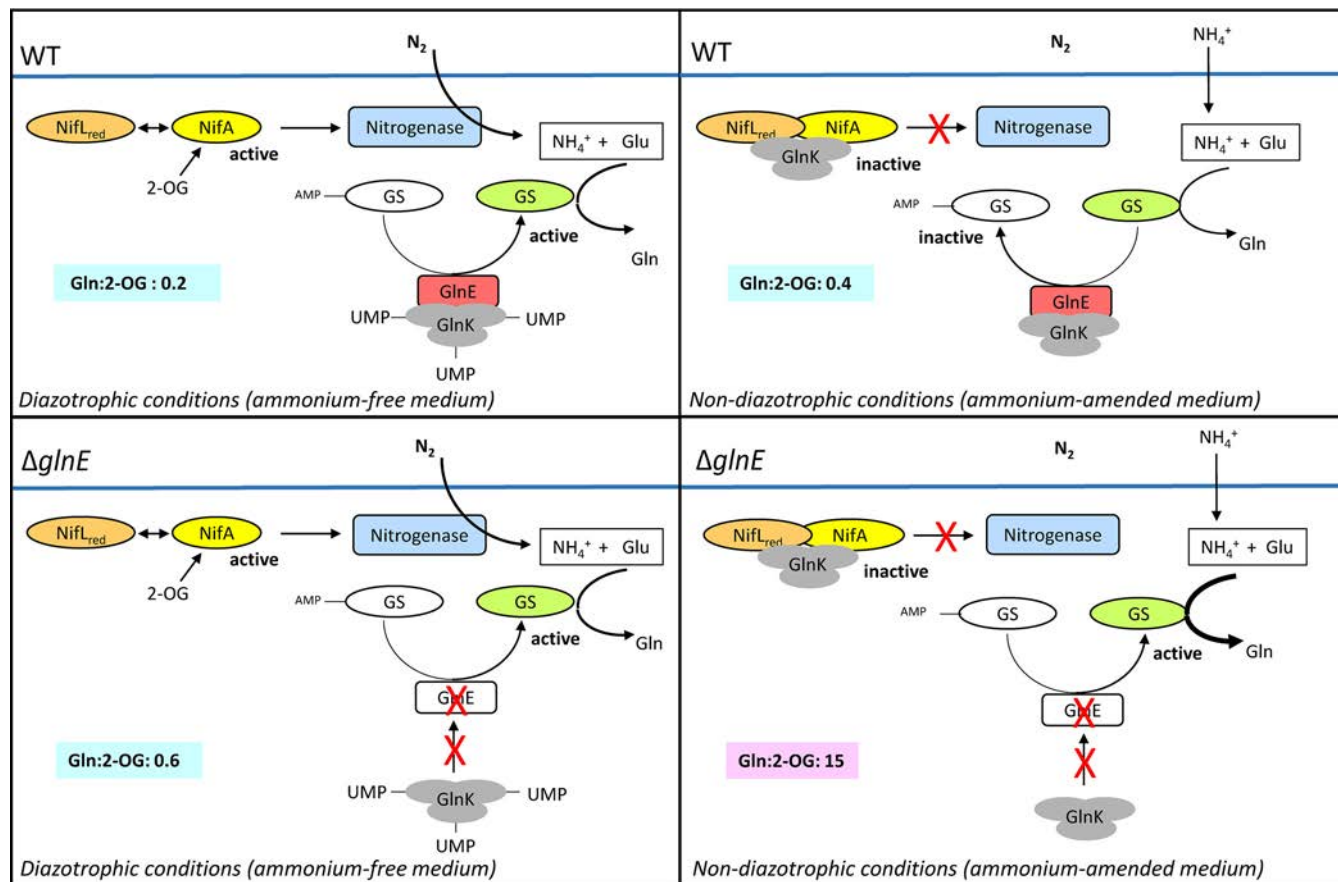


FIG 7 Under diazotrophic conditions (ammonium-free medium), the deadenylation activity of GlnE in the wild-type (WT) strain is favored by high concentrations of 2-OG, as a consequence of saturated uridylylation of GlnK. Under these conditions, 2-OG binds to NifA and thereby prevents protein-protein interaction of NifA and NifL. Under nondiazotrophic conditions (ammonium-amended medium), the adenylation activity of GlnE in the wild-type strain is synergistically activated by GlnK and glutamine (Gln). Under these conditions, GlnK, NifL, and NifA form a ternary complex leading to inactivation of NifA. In the *glnE* mutant strain ($\Delta glnE$), the GlnK regulatory protein is unable to activate GlnE and play its role in promoting GS adenylation, resulting in constitutive activity of GS. The lack of downregulation of GS activity in the *glnE* mutant strain results in high intracellular glutamine levels and severe perturbation of the glutamine-to-2-OG ratio (Gln:2-OG) under nondiazotrophic conditions, which were not observed under diazotrophic conditions. In addition, the mutant was able to grow under diazotrophic conditions at rates comparable to those of the wild-type strain. This observation suggests that the control of nitrogen fixation-specific gene expression at the transcriptional level in response to 2-OG via NifA is sufficiently tight to alone regulate ammonium production at appropriate levels for optimal carbon and nitrogen balance.

tional level by the nitrogen regulatory system, and the biosynthesis of GS is apparently constitutive (6, 7). Consistent with these previous results, only minor changes in the abundance of *glnA* mRNA were observed in the wild-type strain and *glnE* mutant strain in response to the addition of NH_4^+ acetate, and the steady-state *glnA* transcript levels in these strains were not significantly different under diazotrophic conditions.

In all free-living nitrogen-fixing bacteria examined thus far, *nif* transcription is repressed after the addition of NH_4^+ to the culture medium (30). Accordingly, we observed a substantial decrease in steady-state *nifH* mRNA levels 30 min after ammonium upshift in both the wild-type strain and *glnE* mutant strain. This was not accompanied by equivalent decreases in *nifL* and *nifA* transcripts (data not shown) and can be accounted for by posttranslational regulation of the *A. vinelandii* NifL-NifA regulatory system by the nonuridylylated form of GlnK, as reported previously (31–33). Thus, although the absence of adenylyltransferase in the *glnE* mutant strain significantly perturbs the ratio of glutamine to 2-OG, this does not have an obvious influence on the ability of GlnK to regulate the NifL-NifA system in response to an ammonium upshift (Fig. 7). This is potentially because under these conditions, the GlnK-NifL interaction is primarily regulated by glutamine-mediated control of the uridylyltransferase activity of GlnD, rather than the binding of 2-OG to GlnK and NifA (33). Since the

steady-state level of *nifH* mRNA is not altered in the *glnE* mutant strain in the absence of added ammonium, we infer that there is sufficient 2-OG under nitrogen-limiting conditions in the mutant strain to saturate the 2-OG binding site on NifA, hence relieving inhibition by NifL (34, 35). This sophisticated metabolic control of NifA activity facilitates the coupling of NH_4^+ production by nitrogenase to NH_4^+ assimilation, thus preventing the toxic consequences of glutamine overproduction observed when the *glnE* mutant strain is grown in the presence of external NH_4^+ .

In addition to the regulation of *nif* gene expression at the transcriptional level, many diazotrophic bacteria have the capacity to regulate nitrogenase activity directly at the posttranslational level. Rapid switch-off nitrogenase activity has been observed in *A. vinelandii* in response to the addition of NH_4^+ (36), although the molecular mechanism for rapid inhibition of nitrogenase remains unknown. After the addition of 10 mM NH_4^+ acetate, the nitrogenase activities of both the wild-type strain and *glnE* mutant strain declined, as did steady-state *nifH* transcript levels. However, nitrogenase activity in the *glnE* mutant strain was apparently more sensitive to NH_4^+ addition than the wild-type strain, particularly after the addition of 10 mM NH_4^+ acetate. This difference might be accounted for by the altered ratio of glutamine to 2-OG in the *glnE* mutant strain following the ammonium upshift (Fig. 7), which is likely to influence the activity of GlnD and the interaction of GlnK with signal transduction targets other than NifL. In this context, it is interesting to note that the addition of ammonium appears to influence electron transport to nitrogenase in *A. vinelandii* (37). Since rapid switch-off nitrogenase activity in *Azoarcus* sp. strain BH72 involves the interaction of GlnK with the ferredoxin-NAD⁺ reductase (Rnf) complex, a similar mechanism might operate in *A. vinelandii* in which the GlnK-Rnf interaction is modulated by the ratio of glutamine to 2-OG (38). We have demonstrated that GlnE is crucial for the control of GS activity and ultimately essential for *A. vinelandii* viability under excess-ammonium conditions. However, the finding that the *A. vinelandii glnE* mutant strain can grow under diazotrophic conditions at rates comparable to the wild type suggests that high GS activity does not result in feedback regulation of nitrogenase activity. Thus, the sophisticated metabolite regulation of the NifL-NifA system in response to 2-OG and, potentially, the energy charge (39), is sufficiently robust to regulate ammonium production by nitrogenase at appropriate levels for optimal carbon and nitrogen balance. The regulation of nitrogen assimilation and nitrogen fixation is in the vein of biotechnological solutions in which NH_4^+ -excreting diazotrophs are engineered to associate with various crop plants. The *glnE* mutant strain could be used as a tool to examine the threshold of ammonium required and/or tolerated under a specific set of growth conditions, and to identify mutant strains with higher titers of ammonium tolerance.

MATERIALS AND METHODS

Bacterial strains, media, and antibiotics. *E. coli* strain JM109 (Promega, Madison, WI, USA) was grown in Luria-Bertani medium (LB) (40) at 37°C and 250 rpm. For growth curve experiments, *A. vinelandii* strain DJ (wild-type strain; obtained from Dennis Dean, Virginia Tech, VA, USA) (41) and a *glnE* mutant strain (this study) were grown aerobically at 30°C in Burk's sucrose medium (B medium) (7) and Burk's sucrose medium supplemented with 10 or 25 mM NH_4^+ acetate (BN10 medium or BN25 medium, respectively). B medium is an ammonium-free medium; growth in this medium is referred to here as diazotrophic conditions. BN10 and BN25 media are ammonium-amended media; growth in these media is referred to here as nondiazotrophic conditions. Two-hundred-milliliter liquid cultures, contained in 500-ml Erlenmeyer flasks, were incubated on a rotary shaker at 180 rpm. For NH_4^+ acetate shift experiments, *A. vinelandii* strains were grown in 200-ml cultures contained in 500-ml Erlenmeyer flasks and were incubated on a rotary shaker at 180 rpm. After growth at an optical density at 600 nm of 0.5, NH_4^+ acetate was added (10 and 25 mM) as a nitrogen source, and samples were collected at 0, 5, 15, 30, 60, 120, 180, and 300 min after the upshift to excess-nitrogen conditions. Ampicillin and kanamycin were used at 100 $\mu\text{g/ml}$ and 50 $\mu\text{g/ml}$ for *E. coli*, and 100 $\mu\text{g/ml}$ and 5 $\mu\text{g/ml}$ for *A. vinelandii*, respectively. Methionine sulfoximine (MSX) was used on whole cells at a concentration of 1 mM (Sigma-Aldrich, St. Louis, MO, USA).

Construction of the *glnE* deletion mutant. The *glnE* mutant strain was obtained by gene disruption with an antibiotic resistance cassette. DNA fragments containing the 1.5-kb upstream and 1.5-kb downstream genomic region of the *glnE* gene (Avin_44890) were obtained by PCR, using genomic DNA from *A. vinelandii* strain DJ. The primers *glnE*-upstream-F (5'-GGAATTCATATGCCGTTACCGCGGACCGG GCCGTC-3') and *glnE*-upstream-R (5'-CGGGATCCGCTCGTGTCTGATATCGGCCAGACTTCC-3') were used

TABLE 1 List of primers used in this study

Primer	Sequence (5' to 3')
<i>glnE</i> -upstream-F	GGAATTCATATGCCGTTACCGCGGACCGGGCCGTC
<i>glnE</i> -upstream-R	CGGGATCCGCTCGTGTCTGATATCGGCCAGACTTCC
<i>glnE</i> -downstream-F	CGGGATCCGCGGGGCGCCTGCGGGGGCCTGCCGAA
<i>glnE</i> -downstream-R	CCCAAGCTTATCGGCCGGCCCCATTGGGGCCGATGGTGGTCA
A1	AACACCTGGGCGACGAACTC
A2	AACACCTGGGCGACGAACTC
B1	CGCGGATCCGTCGAGCTCCCGGAAGCTTCT
B2	CGCGGATCCTCAGAAGAACTCGTCAAGAAGGCGATAGAAGG
C	GGAAAGTCTGGCCGATATCAGGACACGAGC
<i>glnA</i> -F	TCGAGCCCTCGACCATGCGAG
<i>glnA</i> -R	AGAAGGCGGTGTCGCCGATG
<i>nifH</i> -F	ATCCACTTCGTGCCGCGTGA
<i>nifH</i> -R	CGCGGTATTCGTCCGGCTTGC

for the amplification of a fragment 1.5-kb region upstream of the *glnE* gene, and the primers *glnE*-downstream-F (5'-CGGGATCCGCGGGGCGCCTGCGGGGGCCTGCCGAA-3') and *glnE*-downstream-R (5'-CCCAAGCTTATCGGCCGGCCCCATTGGGGCCGATGGTGGTCA-3') were used for the amplification of a fragment 1.5-kb region downstream of the *glnE* gene (Table 1). The resulting fragments were cloned sequentially in pT7-7 ampicillin-resistant vector (42) using NdeI and BamHI (1.5-kb upstream region) and BamHI and HindIII (1.5-kb downstream region) as restriction cloning sites. The *glnE* gene was disrupted by the insertion of a kanamycin resistance cassette (Kan^r). The KIXX cassette, containing the Kan^r gene (*aph*), was isolated as a 1.5-kb BamHI fragment from pUC4-KIXX (43) (Fig. S1). The cassette was inserted between the 1.5-kb upstream and downstream regions previously cloned in pT7-7 vector using BamHI restriction cloning sites (Fig. S1), which was positioned in the same orientation as the inactivated gene, allowing the transcription of downstream genes. The physical map depicting the plasmids with the corresponding DNA fragments contained and the location of the restriction sites used for the insertion of the antibiotic cassette is shown in Fig. S1. The final construct was transformed into *A. vinelandii* strain DJ, as described previously (44). Kan^r transformants were screened for resistance to ampicillin (Amp^r); ampicillin-susceptible (Amp^s) derivatives were assumed to have arisen from a double-crossover recombination event, such that the wild-type *glnE* gene was replaced by the KIXX-containing DNA (Fig. 2). The chromosomal insertion of the KIXX cassette and deletion of the *glnE* gene were confirmed by PCR using the primers A1/A2, B1/B2, and C/B2 (Table 1 and Fig. S1) and by sequencing.

Protein quantification. *A. vinelandii* cultures (2 ml) were harvested by centrifugation at 14,000 × *g* for 5 min. Cells were disrupted by one cycle of sonication (7 W, 50 s; ultrasonic homogenizer, model 3000; Biologics, Inc., Cary, NC, USA). Protein assays were performed on the same cell lysate for each time point and tested condition. Protein was quantified using the Coomassie protein assay from Thermo Scientific (Waltham, MA, USA). Thirty microliters of sample was mixed with 1.5 ml of Thermo Scientific reagent and incubated at room temperature for 10 min. The absorbance at 595 nm was measured using a spectrophotometer (Thermo Spectronic BioMate 3; Thermo Scientific). The protein content of the sample was calculated using a standard curve (albumin standard used as described by the manufacturer).

Glutamine, glutamate, and 2-OG quantifications. *A. vinelandii* cultures (2 ml) were harvested by centrifugation at 14,000 × *g* for 5 min and immediately frozen in liquid nitrogen. Cell pellets were resuspended in 500 μl of deionized water. Cells were disrupted by one cycle of sonication (7 W, 50 s; ultrasonic homogenizer, model 3000, Biologics, Inc., Cary, NC, USA), and filtered through a centrifugal filter (Amicon Ultra 30K; Millipore, Billerica, MA, USA). Glutamine concentrations were determined using the glutamine colorimetric assay kit (BioVision Incorporated, Milpitas, CA, USA). Glutamate concentrations were determined using the glutamate colorimetric assay kit from BioVision Incorporated. The 2-OG concentrations were determined by the α-ketoglutarate assay kit (Sigma-Aldrich, St. Louis, MO, USA). Appropriate amounts of samples were tested for glutamine and 2-OG quantifications, according to the instructions of the manufacturers, using a 96-well plate reader (SpectraMax Plus 384; Molecular Devices, Sunnyvale, CA, USA).

GS activity assays. An assay for GS activity (45) was used to measure biosynthetic activity (conversion of α-glutamate to γ-glutamyl hydroxamate). The biosynthetic GS activity was used to measure active GS (nonadenylylated enzyme). To determine biosynthetic GS activity, 1 ml of cell culture was collected from *A. vinelandii* cultures and mixed with 100 μl of 10 mg · ml⁻¹ hexadecyltrimethylammonium bromide (CTAB) (46) for 4 min to permeabilize the cells. A 50-μl sample was then removed and used for the determination of GS biosynthetic activity (47).

Nitrogenase activity. To estimate nitrogenase activity, acetylene reduction assays were conducted on freshly grown cultures, as described by Betancourt et al. (48). One milliliter of cell culture was transferred in a 3-ml glass serum vial fitted with a rubber stopper. Two percent of the headspace gas was removed before injecting that same volume of acetylene into the bottle. A 0.5-ml volume was removed from the sample headspace and analyzed for ethylene and ethane using a Shimadzu GC-8A gas chromatograph after 60 min of shaking at 200 rpm and 30°C. The gas chromatograph was fitted on the injector port, a column of 80/100 Porapak Q (6 ft. × 1/8 in.), and a flame ionization detector. The temperatures of the injector, detector, and oven were 90°C, 90°C, and 60°C, respectively. Nitrogenase activity on whole cells was calculated using a standard curve made with ethylene standards.

RNA extraction. Total RNA was isolated from *A. vinelandii* cells using the RNeasy minikit (Qiagen, Valencia, CA, USA), according to the manufacturer's instructions. Genomic DNA was removed from RNA samples by DNase treatment (RNase-free DNase I; Ambion, Grand Island, NY, USA) for 30 min at 37°C (49). The Qiagen RNeasy MinElute kit (Qiagen) was used to purify DNase-treated total RNA from degraded DNA, DNase, contaminating proteins, and potential inhibitors of the reverse transcriptase reaction. The concentration of the eluted RNA was determined with a NanoDrop analyzer.

Reverse transcription reactions. First-strand cDNA synthesis was primed from purified total RNA template using (dT)12–18 primers. The reverse transcription reaction was performed using the reverse transcriptase SuperScript III kit (Invitrogen, Grand Island, NY, USA), as described by the manufacturer. (dT)12–18 primers were annealed to 150 ng of total RNA and extended for 1 h at 50°C using 200 units of SuperScript III reverse transcriptase.

Real-time RT-PCR. Steady-state levels for specific mRNA transcripts from each sample were quantified by absolute real-time RT-PCR using the engine Rotor-Gene Q system (Qiagen). One microliter of single-stranded cDNA from the reverse transcriptase reaction mixture (see above) was used as the template for the real-time PCR experiments. The real-time PCR amplifications were performed using reagents from the DyNAmo SYBR green real-time PCR kit (Finnzymes, Lafayette, CO, USA). Specific primers were designed to amplify gene regions consisting of 90 to 110 nucleotides. The primers used for real-time PCR (*glnA*-F, *glnA*-R, *nifH*-F, and *nifH*-R) are described in Table 1 and were designed using the Primer3 software (50, 51) (Table 1). Amplification by RT-PCR of single products of the expected sizes was verified on 2% (wt/vol) agarose gels, and the specificity of PCR products was verified by sequencing. Melting curve analyses were performed on all PCR products to ensure that single DNA species were amplified. Real-time PCR amplifications were performed using the following cycling parameters: an initial single step at 95°C for 10 min (denaturation) was followed by 40 cycles of the following: 94°C for 10 s (denaturation), 60°C for 20 s (primer annealing for *glnA* and *nifH* genes), and 72°C for 30 s (elongation). A final single step at 72°C for 1 min followed these 40 cycles. Absolute quantification (52) of each specific RNA was determined among all samples collected at the following time points: 0, 5, 30, and 180 min.

SUPPLEMENTAL MATERIAL

Supplemental material for this article may be found at <https://doi.org/10.1128/AEM.00808-17>.

SUPPLEMENTAL FILE 1, PDF file, 0.3 MB.

ACKNOWLEDGMENTS

This work was supported by the National Science Foundation grant no. NSF-1331098.

We thank Philip S. Poole for collaboration on the research herein.

REFERENCES

- van Heeswijk WC, Westerhoff HV, Booger FC. 2013. Nitrogen assimilation in *Escherichia coli*: putting molecular data into a systems perspective. *Microbiol Mol Biol Rev* 77:628–695. <https://doi.org/10.1128/MMBR.00025-13>.
- Poole P, Allaway D. 2000. Carbon and nitrogen metabolism in *Rhizobium*. *Adv Microb Physiol* 43:117–163. [https://doi.org/10.1016/S0065-2911\(00\)43004-3](https://doi.org/10.1016/S0065-2911(00)43004-3).
- Bellion E, Tan F. 1987. An NAD⁺-dependent alanine dehydrogenase from a methylotrophic bacterium. *Biochem J* 244:565–570.
- Kennedy C, Toukdarian A. 1987. Genetics of azotobacters: applications to nitrogen fixation and related aspects of metabolism. *Annu Rev Microbiol* 41:227–258. <https://doi.org/10.1146/annurev.mi.41.100187.001303>.
- Kleinschmidt JA, Kleiner D. 1981. Relationships between nitrogenase, glutamine synthetase, glutamine, and energy charge in *Azotobacter vinelandii*. *Arch Microbiol* 128:412–415. <https://doi.org/10.1007/BF00405923>.
- Santero E, Luque F, Medina JR, Tortolero M. 1986. Isolation of *ntrA*-like mutants of *Azotobacter vinelandii*. *J Bacteriol* 166:541–544. <https://doi.org/10.1128/jb.166.2.541-544.1986>.
- Toukdarian A, Kennedy C. 1986. Regulation of nitrogen metabolism in *Azotobacter vinelandii*: isolation of *ntr* and *glnA* genes and construction of *ntr* mutants. *EMBO J* 5:399–407.
- Lepo JE, Wyss O, Tabita FR. 1982. Regulation and biochemical characterization of the glutamine synthetase of *Azotobacter vinelandii*. *Biochim Biophys Acta* 704:414–421. [https://doi.org/10.1016/0167-4838\(82\)90062-0](https://doi.org/10.1016/0167-4838(82)90062-0).
- Ginsburg A. 1972. Glutamine synthetase of *Escherichia coli*: some physical and chemical properties. *Adv Prot Chem* 26:1–79. [https://doi.org/10.1016/S0065-3233\(08\)60139-4](https://doi.org/10.1016/S0065-3233(08)60139-4).
- Levine RL, Mosoni L, Berlett BS, Stadtman ER. 1996. Methionine residues as endogenous antioxidants in proteins. *Proc Natl Acad Sci U S A* 93:15036–15040. <https://doi.org/10.1073/pnas.93.26.15036>.
- Liaw SH, Villafranca JJ, Eisenberg D. 1993. A model for oxidative modification of glutamine synthetase, based on crystal structures of mutant H269N and the oxidized enzyme. *Biochemistry* 32:7999–8003. <https://doi.org/10.1021/bi00082a022>.
- Almassy RJ, Janson CA, Hamlin R, Xuong NH, Eisenberg D. 1986. Novel subunit-subunit interactions in the structure of glutamine synthetase. *Nature* 323:304–309. <https://doi.org/10.1038/323304a0>.
- Gill HS, Pfluegl GMU, Eisenberg D. 2002. Multicopy crystallographic refinement of a relaxed glutamine synthetase from *Mycobacterium tuberculosis* highlights flexible loops in the enzymatic mechanism and its regulation. *Biochemistry* 41:9863–9872. <https://doi.org/10.1021/bi020254s>.
- Rhee SG, Park SC, Koo JH. 1985. The role of adenylyltransferase and uridylyltransferase in the regulation of glutamine synthetase in *Escherichia coli*. *Curr Top Cell Regul* 27:221–232. <https://doi.org/10.1016/B978-0-12-152827-0.50026-8>.
- Stadtman ER. 2001. The story of glutamine synthetase regulation. *J Biol Chem* 276:44357–44364. <https://doi.org/10.1074/jbc.R100055200>.
- Fink D, Falke D, Wohlleben W, Engels A. 1999. Nitrogen metabolism in *Streptomyces coelicolor* A3(2): modification of glutamine synthetase I by an adenylyltransferase. *Microbiology* 145:2313–2322. <https://doi.org/10.1099/00221287-145-9-2313>.
- Kustu S, Hirschman J, Burton D, Jelesko J, Meeks JC. 1984. Covalent modification of bacterial glutamine synthetase: physiological significance. *Mol Gen Genet* 197:309–317. <https://doi.org/10.1007/BF00330979>.
- Foor F, Janssen KA, Magasanik B. 1975. Regulation of synthesis of glutamine synthetase by adenylylated glutamine synthetase. *Proc Natl Acad Sci U S A* 72:4844–4848. <https://doi.org/10.1073/pnas.72.12.4844>.

19. Espin G, Alvarez-Morales A, Cannon F, Dixon R, Merrick M. 1982. Cloning of the *glnA*, *ntrB* and *ntrC* genes of *Klebsiella pneumoniae* and studies of their role in regulation of the nitrogen fixation (*nif*) gene cluster. *Mol Gen Genet* 186:518–524. <https://doi.org/10.1007/BF00337959>.
20. Colnaghi R, Rudnick P, He L, Green A, Yan D, Larson E, Kennedy C. 2001. Lethality of *glnD* null mutations in *Azotobacter vinelandii* is suppressible by prevention of glutamine synthetase adenylation. *Microbiology* 147: 1267–1276. <https://doi.org/10.1099/00221287-147-5-1267>.
21. Kleinschmidt JA, Kleiner D. 1978. The glutamine synthetase from *Azotobacter vinelandii*: purification, characterization, regulation, and localization. *Eur J Biochem* 89:51–60. <https://doi.org/10.1111/j.1432-1033.1978.tb20895.x>.
22. Liaw SH, Eisenberg D. 1994. Structural model for the reaction mechanism of glutamine synthetase, based on five crystal structures of enzyme-substrate complexes. *Biochemistry* 33:675–681. <https://doi.org/10.1021/bi00169a007>.
23. Ortiz-Marquez JCF, Do Nascimento M, Curatti L. 2014. Metabolic engineering of ammonium release for nitrogen-fixing multispecies microbial cell-factories. *Metab Eng* 23:154–164. <https://doi.org/10.1016/j.ymben.2014.03.002>.
24. Zhang Y, Pohlmann EL, Conrad MC, Roberts GP. 2006. The poor growth of *Rhodospirillum rubrum* mutants lacking PII proteins is due to an excess of glutamine synthetase activity. *Mol Microbiol* 61:497–510. <https://doi.org/10.1111/j.1365-2958.2006.05251.x>.
25. Jonsson A, Nordlund S, Teixeira PF. 2009. Reduced activity of glutamine synthetase in *Rhodospirillum rubrum* mutants lacking the adenylyltransferase GlnE. *Res Microbiol* 160:581–584. <https://doi.org/10.1016/j.resmic.2009.09.003>.
26. Yasid NA, Rolfe MD, Green J, Williamson MP. 2016. Homeostasis of metabolites in *Escherichia coli* on transition from anaerobic to aerobic conditions and the transient secretion of pyruvate. *Royal Soc Open Sci* 3:160187. <https://doi.org/10.1098/rsos.160187>.
27. Yuan J, Doucette CD, Fowler WU, Feng X-J, Piazza M, Rabitz HA, Wingreen NS, Rabinowitz JD. 2009. Metabolomics-driven quantitative analysis of ammonia assimilation in *E. coli*. *Mol Syst Biol* 5:302. <https://doi.org/10.1038/msb.2009.60>.
28. Basan M, Hui S, Okano H, Zhang Z, Shen Y, Williamson JR, Hwa T. 2015. Overflow metabolism in *Escherichia coli* results from efficient proteome allocation. *Nature* 528:99–104. <https://doi.org/10.1038/nature15765>.
29. Hart Y, Madar D, Yuan J, Bren A, Mayo AE, Rabinowitz JD, Alon U. 2011. Robust control of nitrogen assimilation by a bifunctional enzyme in *E. coli*. *Mol Cell* 41:117–127. <https://doi.org/10.1016/j.molcel.2010.12.023>.
30. Dixon R, Kahn D. 2004. Genetic regulation of biological nitrogen fixation. *Nat Rev Microbiol* 2:621–631. <https://doi.org/10.1038/nrmicro954>.
31. Little R, Reyes-Ramirez F, Zhang Y, van Heeswijk WC, Dixon R. 2000. Signal transduction to the *Azotobacter vinelandii* NIFL–NIFA regulatory system is influenced directly by interaction with 2-oxoglutarate and the PII regulatory protein. *EMBO J* 19:6041–6050. <https://doi.org/10.1093/emboj/19.22.6041>.
32. Rudnick P, Kunz C, Gunatilaka MK, Hines ER, Kennedy C. 2002. Role of GlnK in NifL-mediated regulation of NifA activity in *Azotobacter vinelandii*. *J Bacteriol* 184:812–820. <https://doi.org/10.1128/JB.184.3.812-820.2002>.
33. Little R, Colombo V, Leech A, Dixon R. 2002. Direct interaction of the NifL regulatory protein with the GlnK signal transducer enables the *Azotobacter vinelandii* NifL–NifA regulatory system to respond to conditions replete for nitrogen. *J Biol Chem* 277:15472–15481. <https://doi.org/10.1074/jbc.M112262200>.
34. Little R, Dixon R. 2003. The amino-terminal GAF domain of *Azotobacter vinelandii* NifA binds 2-oxoglutarate to resist inhibition by NifL under nitrogen-limiting conditions. *J Biol Chem* 278:28711–28718. <https://doi.org/10.1074/jbc.M301992200>.
35. Martinez-Argudo I, Little R, Dixon R. 2004. A crucial arginine residue is required for a conformational switch in NifL to regulate nitrogen fixation in *Azotobacter vinelandii*. *Proc Natl Acad Sci U S A* 101:16316–16321. <https://doi.org/10.1073/pnas.0405312101>.
36. Klugkist J, Haaker H. 1984. Inhibition of nitrogenase activity by ammonium chloride in *Azotobacter vinelandii*. *J Bacteriol* 157:148–151.
37. Laane C, Krone W, Konings W, Haaker H, Veeger C. 1980. Short-term effect of ammonium chloride on nitrogen fixation by *Azotobacter vinelandii* and by bacteroids of *Rhizobium leguminosarum*. *Eur J Biochem* 103:39–46. <https://doi.org/10.1111/j.1432-1033.1980.tb04286.x>.
38. Sarkar A, Köhler J, Hurek T, Reinhold-Hurek B. 2012. A novel regulatory role of the Rnf complex of *Azoarcus* sp. strain BH72. *Mol Microbiol* 83:408–422. <https://doi.org/10.1111/j.1365-2958.2011.07940.x>.
39. Perry S, Shearer N, Little R, Dixon R. 2005. Mutational analysis of the nucleotide-binding domain of the anti-activator NifL. *J Mol Biol* 346: 935–949. <https://doi.org/10.1016/j.jmb.2004.12.033>.
40. Bertani G. 1951. Studies on lysogeny. I. The mode of phage liberation by lysogenic *Escherichia coli*. *J Bacteriol* 62:293–300.
41. Setubal JC, dos Santos P, Goldman BS, Ertesvåg H, Espin G, Rubio LM, Valla S, Almeida NF, Balasubramanian D, Cromes L, Curatti L, Du Z, Godsy E, Goodner B, Hellner-Burris K, Hernandez JA, Houmiel K, Imperial J, Kennedy C, Larson TJ, Latreille P, Ligon LS, Lu J, Mærk M, Miller NM, Norton S, O'Carroll IP, Paulsen I, Raulfs EC, Roemer R, Rosser J, Segura D, Slater S, Stricklin SL, Studholme DJ, Sun J, Viana CJ, Wallin E, Wang B, Wheeler C, Zhu H, Dean DR, Dixon R, Wood D. 2009. Genome sequence of *Azotobacter vinelandii*, an obligate aerobe specialized to support diverse anaerobic metabolic processes. *J Bacteriol* 191:4534–4545. <https://doi.org/10.1128/JB.00504-09>.
42. Tabor S, Richardson CC. 1985. A bacteriophage T7 RNA polymerase/promoter system for controlled exclusive expression of specific genes. *Proc Natl Acad Sci U S A* 82:1047–1048.
43. Brewin B, Woodley P, Drummond M. 1999. The basis of ammonium release in *nifL* mutants of *Azotobacter vinelandii*. *J Bacteriol* 181: 7356–7362.
44. Page WJ, von Tigerstrom M. 1978. Induction of transformation competence in *Azotobacter vinelandii* iron-limited cultures. *Can J Microbiol* 24:1590–1594. <https://doi.org/10.1139/m78-254>.
45. Bressler SL, Ahmed SI. 1984. Detection of glutamine synthetase activity in marine phytoplankton: optimization of the biosynthetic assay. *Mar Ecol Prog Ser* 14:207–217. <https://doi.org/10.3354/meps014207>.
46. Bender RA, Janssen KA, Resnick AD, Blumenberg M, Foor F, Magasanik B. 1977. Biochemical parameters of glutamine synthetase from *Klebsiella aerogenes*. *J Bacteriol* 129:1001–1009.
47. Robinson P, Neelon K, Schreiber HJ, Roberts MF. 2001. β -Glutamate as a substrate for glutamine synthetase. *Appl Environ Microbiol* 67: 4458–4463. <https://doi.org/10.1128/AEM.67.10.4458-4463.2001>.
48. Betancourt DA, Loveless TM, Brown JW, Bishop PE. 2008. Characterization of diazotrophs containing Mo-independent nitrogenases, isolated from diverse natural environments. *Appl Environ Microbiol* 74: 3471–3480. <https://doi.org/10.1128/AEM.02694-07>.
49. Huang Z, Fasco MJ, Kaminsky LS. 1996. Optimization of DNase I removal of contaminating DNA from RNA for use in quantitative RNA-PCR. *Biotechniques* 20:1012–1014.
50. Koressaar T, Remm M. 2007. Enhancements and modifications of primer design program Primer3. *Bioinformatics* 23:1289–1291. <https://doi.org/10.1093/bioinformatics/btm091>.
51. Untergasser A, Cutcutache I, Koressaar T, Ye J, Faircloth BC, Remm M, Rozen SG. 2012. Primer3—new capabilities and interfaces. *Nucleic Acids Res* 40:e115. <https://doi.org/10.1093/nar/gks596>.
52. Whelan JA, Russell NB, Whelan MA. 2003. A method for the absolute quantification of cDNA using real-time PCR. *J Immunol Methods* 278: 261–269. [https://doi.org/10.1016/S0022-1759\(03\)00223-0](https://doi.org/10.1016/S0022-1759(03)00223-0).